A very low-complexity filter lookup-table design with non-uniform spacing for SOA linearization

Mohamad Younes, Mihai Telescu, Stéphane Azou, Pascal Morel, Noël Tanguy

IET Research Journals

Submission Template for IET Research Journal Papers

IET Journals
The Institution of Engineering and Technology

A very low-complexity filter lookup-table design with non-uniform spacing for SOA linearization

ISSN 1751-8644
doi: 0000000000
www.ietdl.org

Mohamad Younes[1], *Mihai Telescu*[1], *Stéphane Azou*[2], *Pascal Morel*[2], *Noël Tanguy*[1]

[1] *Univ Brest, Lab-STICC, CNRS, UMR 6285, F-29200 Brest, France*
[2] *ENIB, Lab-STICC, CNRS, UMR 6285, Brest, France*

Abstract: Nonlinearities introduced by power amplifiers in communication systems have been a subject of interest for industry and academia for a long time. On one hand the search for increased range intrinsically incites operators to boost input power. On the other hand this leads to stronger nonlinear phenomena in amplifiers which in turn increase the bit error rate. The situation led to the emergence of digital predistortion algorithms that compensate the power-amplifier's nonlinearities and improve the overall performance of the link. A rich corpus of literature exists on this topic but it mainly addresses wireless microwave networks. The case of digital predistortion specifically tailored for optical communications is much less explored. This paper focuses on predistortion via filter-lookup-tables and tackles the issue of non-uniform spacing. The work is mainly aimed at CO-OFDM systems including low-cost semiconductor optical amplifiers.

1 Introduction

For decades, telecommunications have been a highly competitive field of technology with actors racing for high data throughput, service versatility and flexibility and increased mobility. Orthogonal frequency-division multiplexing (OFDM) has been codified in several extant standards (ADSL, WiMAX, Wi-Fi, LTE, DVB, ...) and constitutes one of the solutions that many industry actors favor. This paper focuses on the case of Coherent Optical OFDM (CO-OFDM) and particularly on a scenario including semiconductor optical amplifiers (SOA). This scenario has been investigated in recent literature [1, 2] and is appealing because of the SOA's large optical bandwidth, integration capability and reduced cost. However, SOAs are also known to exhibit nonlinear effects, resulting from their fast gain dynamics. In fact, if an SOA is driven by a constant bias current with a non-constant envelope input signal at its input, a large decrease of the carrier density may occur within its active region. This is explained by the fact that a higher power signal interacts with a larger number of excited electrons in the conduction band, thus resulting in depletion of carrier density and SOA gain [3]. This translates in a variety of nonlinearities including Self-Gain and Self-Phase Modulations (SGM, SPM), Cross-Gain and Cross-Phase Modulations (XGM, XPM), Four-Wave Mixing (FWM), amplitude-phase coupling and gain compression. It should be noted that nonlinear effects are associated with all power amplifiers (PA) and several linearization techniques have been proposed in order to circumvent or at least alleviate this problem [4]. Baseband digital predistortion (DPD) is a well-established, efficient solution in the wireless communication community [5] and has also been considered, more recently, in optical communications [6, 7]. The general idea is that since the PA introduces a nonlinear transformation of the data signal, one may design a specific scheme that introduces the inverse transformation and compensates this undesirable side-effect. Predistortion schemes may feature or, on the contrary, lack memory. Memoryless systems are popular because of their simplicity [5, 8–11], one of the most common solutions being simple lookup-tables mapping complex gain factors [10–17]. In their most basic implementation lookup-tables use uniformly spaced entries. Pioneering work by Cavers [11] showed that uniformly spaced amplitude mapping usually leads to better performance than power mapping. More recent literature focused on non-uniform spacing schemes and proved that performance may be further enhanced by such approaches without increasing system complexity. In [11–17] input amplitude is fed into a companding function leading to the computation of improved LUT indexes reducing inter-modulation distortions. An analytical solution for optimal non-uniform spacing was proposed in [11]. It advocates the use of entries spaced according to an intricate law depending on the PA's gain function and on the probability density function (PDF) of the input signal. Subsequent work in [16] led to a more robust solution where spacing only depends on the PA's gain function. Papers [15], [17], [18] also propose the interpolation of LUT entries with [15] being remarkable in its analytic approach designed to minimize interpolation error.

Filter lookup-tables (FLUT) are an improvement of the LUT concept with the potential to compensate dynamic nonlinearities. The structure of FLUTs has only been studied with uniformely spaced table entries and uniformely spaced filter codebooks[19, 20]. In this paper we introduce non-uniform spacing solutions leading to a significant improvement in terms of error-vector magnitude (EVM). We rely on an algorithm seeking to minimize the error due to the linear interpolation between table entries. Optimal spacing results as a function of the PDF of the input signal and the inverse model of the amplifier as shown in [15]. A better rejection of residual nonlinear distortions is thus obtained. But the main theoretical novelty is related to the filter codebook, improved according to an original method. As a general rule, with a FLUT, the magnitude range of the input signal is divided into bins and each filter in the codebook corresponds to one bin. The novel solution proposed in the present paper seeks to ensure that the number of input samples present in each interval is the same. A non-uniformly spaced codebook results leading to a further improvement in terms of EVM. Sections 2 and 3 present the theoretical principles of linearly interpolated LUT and FLUT predistorters with both conventional and original spacing solutions. Section 4 reports the numerical results showing that the newly proposed approaches perform best.

2 System model and FLUT Predistortion

Throughout this paper we consider a coherent OFDM transmitter with the PA acting as a power booster. The transmitter and receiver are standard, with the exception of one block dedicated to linearization (predistorter FLUT)[19].

Predistortion uses a simple principle. The undesirable effects introduced by a nonlinear element within the link (usually the PA)

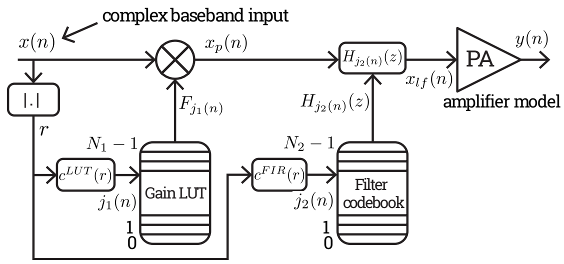

Fig. 1: Complex gain FLUT predistortion followed by PA.

can be compensated by another nonlinear block placed upstream. The latter should idealy implement the inverse nonlinear function. Figure 1 shows the cascaded baseband DPD (FLUT) and PA. Note that the FLUT itself is made up of two main blocks: a LUT and a filter codebook as described in [19, 20]. The LUT, powered by the complex envelope $x(n)$ of the input modulated signal, generates the predistorted signal $x_p(n)$ according to $x_p = xF_{j_1(n)}(r)$, where $r = |x|$ and $F_{j_1(n)}$ is the complex gain of the LUT for index $j_1(n) \in [0, N_1 - 1]$. In the elementary case of a LUT-based predistortion (without the filter stage), the output of the amplifier $y(n)$ is then $y = x_p G(r_p)$, where $r_p = |x_p|$ and $G(r_p)$ is the complex gain of a memoryless amplifier presented in equation 1. Ideally, the LUT is optimized to produce a simple linear gain (K) and an arbitrary constant phase shift (Φ_0), so that:

$$G(r|f(r)|)f(r) = K\exp(i\Phi_0) \tag{1}$$

where f denotes the amplifier inverse model.

If the amplifier has negligible dynamics, the standalone LUT should be sufficient to compensate the undesired nonlinear distortion it introduces. As seen later on in the paper this favorable scenario is not always realistic. The parameters of the FLUT are identified using a hybrid approach. The entries of the LUT are computed by direct learning while an indirect method is used to estimate the coefficients of the filters (see [19] for details). Functions $c^{LUT}(r)$ and $c^{FIR}(r)$, shown in figure 1, control the way in which entries are spaced within the LUT and the codebook respectively. By mathematical convention we consider that the gain K of the amplifier is normalized to the unit. We also consider that the function $c(r)$ ($c^{LUT}(r)$ or $c^{FIR}(r)$) is defined for the interval $r \in [0, 1]$ and is monotonically increasing so that $c'(r) > 0, \forall r \in [0, 1]$ over this interval. Note that the width of the resulting bins is inversely proportional to the first order derivative of the spacing function $c(r)$ and to the number of inputs N (N_1 or N_2) as follows [5, 11–16, 19–21]:

$$d = \frac{1}{c'(r)N}. \tag{2}$$

Several techniques for linearly interpolated LUT spacing have been studied. TABLE 1 illustrates a set of conventional methods. It should be noted that A-law, originally developed for speech processing is uncommon in digital predistortion applications. It is nonetheless a viable alternative to μ-law. None of these techniques takes into account the characteristic of the PA, modulation format nor signal statistics. This is their main limitation.

3 Improved FLUT Spacing

3.1 An optimal LUT spacing

To the authors' knowledge there are no published attempts to optimize spacing in a FLUT predistorter. However, several recent advances exist in the optimization of LUT spacing and constitute a valuable resource for the present paper. One strategy is to rely on an analytical model of the PA[11, 14] while another approach advocates the estimation of an inverse function [15–17, 21]. In both cases knowledge of the PDF of the input signal is required. Compared to the previously mentioned references, in the present paper a purely behavioral inverse model of the amplifier is adopted. This general approach requires no hypothesis regarding the physical nature of the amplifier, by modeling its AM/AM (amplitude-to-amplitude modulation) and AM/PM (amplitude-to-phase modulation) characteristics as a result of simple polynomial identification.

Table 1 Standard spacing functions with their derivatives.

Spacing scheme	Spacing function $c(r)$	Derivative of the spacing function
Amplitude [11–17]	r	1
Power [11, 16, 17]	r^2	$2r$
μ-law [11]	$\frac{\ln(1+\mu r)}{\ln(1+\mu)}$	$\frac{\mu}{\ln(1+\mu)}\frac{1}{1+\mu r}$
A-law	$\frac{Ar}{1+\ln(A)}, r < \frac{1}{A}$ $\frac{1+\ln(Ar)}{1+\ln(A)}, r \geq \frac{1}{A}$	$\frac{A}{1+\ln(A)}, r < \frac{1}{A}$ $\frac{1}{1+\ln(A)}\frac{1}{r}, r \geq \frac{1}{A}$

Let the PA be considered as a purely static block at this stage and let f denote its inverse function. It is reasonable to assume that f may be expressed as a function of two distinct polynomials $\{f_{AM-AM}(r), f_{AM-PM}(r)\}$ translating the amplitude and phase distortions respectively:

$$f(r) = f_{AM-AM}(r)\exp(if_{AM-PM}(r)) \tag{3}$$

with

$$f_{AM-AM}(r) = \sum_{l=0}^{L_1} \beta_l r^l, \tag{4}$$

$$f_{AM-PM}(r) = \sum_{l=0}^{L_2} \gamma_l r^l \tag{5}$$

and $r = |x|$. At this stage LUT spacing may be optimized using the method presented in [15] which relies on a general principle of quantization theory [12, 21]. The lookup-table approach intrinsically introduces an approximation of r which is replaced by a finite number of bins r_k with $k = 0, ..., N_1 - 1$. Let the width of a bin be defined as $d = r_{k+1} - r_k$. It follows that for a complex input x of magnitude r falling within the bin a bounded approximation error will be introduced so that $r = r_k + \epsilon_r$ with $0 < \epsilon_r < d$. This error will also impact function f that will be approximated by

$$\check{f}(r) = f(r) + \epsilon_f \tag{6}$$

with ϵ_f being the resulting error. Assuming the bins are narrow enough, a good estimation of ϵ_f may be computed, hence we may consider it known. It follows that the true output signal of the amplifier can be analytically written as

$$\check{y} = G(r|\check{f}(r)|)\check{f}(r)x \quad (7)$$

whereas the desired output signal is $y = G(r|f(r)|)f(r)x$. Optimum spacing may then be defined as minimizing $E(|\epsilon_y|^2)$ with $\epsilon_y = y - \check{y}$. Following the procedure in [15] the analytic expression of the derivative of the optimum spacing function $c_{opt}(r)$ can be obtained and written as

$$c'_{opt}(r) = \frac{w^{\frac{1}{5}}(r)}{\int_0^1 w^{\frac{1}{5}}(r)dr} \quad (8)$$

Function $w(r)$ is defined as

$$w(r) = |\psi(r)|^2 p(r) \quad (9)$$

where $p(r)$ is the PDF of the input signal and $\psi(r)$ is given by

$$\psi(r) = \frac{f''(r)f^*(r) + ir\text{Imag}(f'^*(r)f''(r))}{|f(r)|^2 + r\text{Real}(f^*(r)f'(r))}x \quad (10)$$

Replacing c'_{opt} in (2) yields for $r = r_k$ with $k = 0...N_1 - 1$ a new set of bins of varying width. This result obtained by Ba *et al.* [15] is of paramount importance in designing powerful predistortion linearly interpolated LUTs.

3.2 Improved filter Codebook spacing

Unfortunately for several applications, standalone LUTs make poor predistorters as one also wants to compensate for dynamic distortions. Predistorters thus have to be upgraded to include memory hence the addition of a filter codebook as described in figure 1.

Let the j_2th FIR in the codebook be defined by its transfer function $H_{j_2}(z)$ and impulse response $h_{j_2}(k)$ which are linked by the classic relation

$$H_{j_2}(z) = \sum_{k=0}^{L-1} h_{j_2}(k)z^{-k} \quad (11)$$

The input-output relation of the global filter-lookup-table system is given by

$$x_{lf}(n) = \sum_{k=0}^{L-1} h_{j_2(n)}(k)x_p(n-k) \quad (12)$$

Recalling that x_p is the output of the LUT block and replacing its expression in (12) yields

$$x_{lf}(n) = \sum_{k=0}^{L-1} h_{j_2(n)}(k)F_{j_1(n-k)}x(n-k) \quad (13)$$

At this point, spacing, which may be considered a solved problem for the LUT, becomes an issue for the codebook. A trivial approach would be to optimize the spacing for the LUT and use the same bins for the filter codebook. In other words the index functions $j_1(n)$ and $j_2(n)$ in figure 1 could be considered identical (and $N_1 = N_2$). This solution was tested and the results are presented in the following section but the authors also propose another approach which leads to better performance and constitutes the main theoretical development in the present paper. Consider the scenario of a relatively small number of uniformly spaced bins. The probability of an input value falling within some bins may have a low probability of occurrence, as illustrated in figure 2 (PDF with a small tail on the right-hand side). Hence, during the learning stage, the estimation of filter coefficients for high values of j_2 will be based on few samples and will thus be inaccurate. This is extremely inconvenient since it is

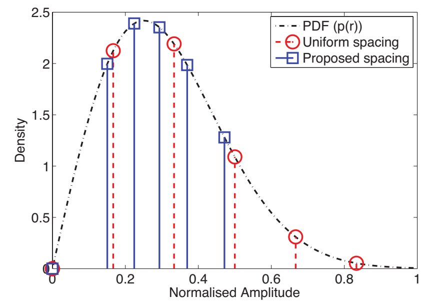

Fig. 2: PDF as a function of the input amplitude of the codebook based on classic and proposed spacing ($N_2 = 6$); case of an OFDM signal with $N_{sc} = 128$ subcarriers, clipped and then normalized.

particularly at high amplitudes that nonlinear distortions are powerful. Consequently, a well chosen empirical criterion for non-uniform spacing would be the equi-distribution of samples over the different bins. The specific case of an OFDM signal is subsequently considered. It is known that the PDF in this case follows a Rayleigh law with

$$p(r) = 2\frac{r}{\sigma^2}\exp(-\frac{r^2}{\sigma^2}) \quad (14)$$

In practice the cumulative probability of input magnitude exceeding a certain value is so low that the tail on the right-hand side of the Rayleigh PDF will always be clipped. Futhermore we also consider that the signal is normalized in order to be inline with previous literature. We recall that the very definition of the PDF implies $\int_0^1 p(r) = 1$. We seek to insure that the probability for an input sample to fall within a specific bin is the same for all bins, i.e.

$$\int_{q_{j_2}}^{q_{j_2+1}} p(r)\,dr = \frac{1}{N_2}, \text{with } j_2 = 0, ..., N_2 - 1 \quad (15)$$

The spacing can then be expressed by an iterative law with the quantum for bin $j_2 + 1$ depending on the quantum for bin j_2.

$$q_{j_2+1} = \sigma\sqrt{-\log(-\frac{1}{N_2} + \exp(-\frac{q_{j_2}^2}{\sigma^2}))}, \quad (16)$$

with $j_2 = 1, ..., N_2$ and $q_0 = 0$.

Thus the width of the jth bin is defined by the difference

$$d_{opt}^{FIR} = q_{j_2+1} - q_{j_2} \quad (17)$$

Using the analytical expression of the PDF to improve spacing is elegent however in practice this is not always possible. Quite often OFDM systems include companding/decompanding blocks in order to reduce peak-to-average-power-ratio (PAPR) [20] in which case the PDF no longer follows a Rayleigh distribution. Nonetheless, the principle of equi-distribution of samples over the various bins holds and it can be enforced empirically by studying the histogram of the input samples.

4 Performance Evaluation

4.1 Application example: CO-OFDM System

While the theoretical principles described above are general the authors tested the approach in the specific framework of a coherent optical OFDM (CO-OFDM) transmission system. The implementation of such links using semiconductor optical amplifiers (SOA) of moderate cost has attracted significant attention in recent years and appears to be promising (see [20], [22] and the references therein).

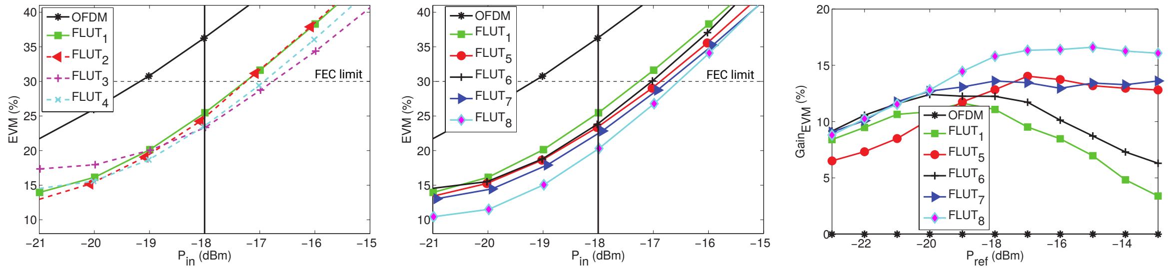

(a) Performances for an identification power P_{ref} = -18 dBm of the standard spacing methods.

(b) Performances for an identification power P_{ref} = -18 dBm of the alternative spacing methods.

(c) Effect of identification power on alternative spacing methods.

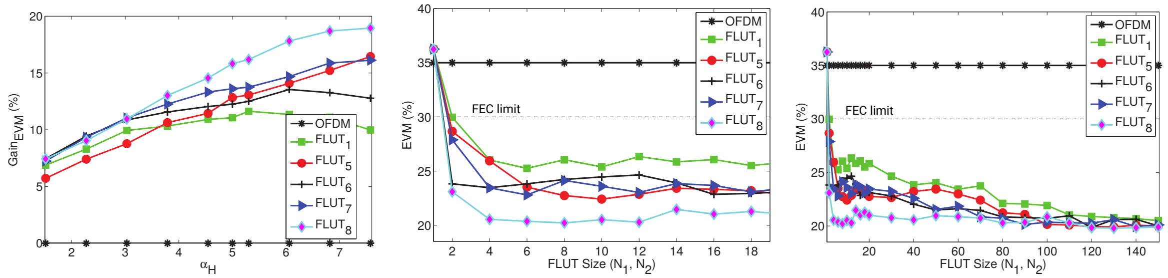

(d) Effect of PA Henry factor, for P_{ref} = -18 dBm.

(e) Effect of FLUT input size, for P_{ref} = -18 dBm.

(f) Effect of FLUT input size, for P_{ref} = -18 dBm.

Fig. 3: Standard and alternative spacing methods.

In the present study, a commercial 750 μm SOA (INPHENIX-IPSAD1501) is considered. The CO-OFDM link was simulated using a hybrid Matlab-ADS implementation that has already been validated by experiments [22]. The modulation format is quadrature phase shift keying (QPSK) with 128 subcarriers and 3 GHz bandwidth, resulting in a 5 Gb/s transmission. The SOA is powered by a bias current of 200 mA, resulting in a gain of 19 dB and a noise factor of 7 dB for a laser wavelength of 1540 nm. It should be emphasized that FWM may be considered as the prominent nonlinear effect in SOAs if multicarrier modulation are employed, with the nonlinear distortion depending both on the subcarrier spacing and on injected optical power. The FWM products become weaker compared to the main signal when the frequency interval increases. Note that the scenario proposed here can be considered challenging, from the linearization point of view, once the optical power injected into the SOA exceeds -21 dBm (saturated region).

Table 2 Spacing methods used in the paper. The LUT optimal spacing refers to the method described in [15].

Spacing scheme	LUT spacing	Filter Codebook spacing
$FLUT_1$	uniform (amplitude)	uniform (amplitude)
$FLUT_2$	uniform (power)	uniform (power)
$FLUT_3$	non uniform (μ-law)	non uniform (μ-law)
$FLUT_4$	non uniform (A-law)	non uniform (A-law)
$FLUT_5$	follows codebook	improved
$FLUT_6$	optimal	follows LUT
$FLUT_7$	optimal	uniform (amplitude)
$FLUT_8$	optimal	improved

4.2 Non-uniform spacing methods

The authors conducted extensive testing of various FLUT configurations listed in TABLE 2 with linearly interpolated LUT(s). The most basic variants use uniform amplitude spacing ($FLUT_1$) and uniform power spacing ($FLUT_2$). Conventional non-uniform (NU) spacing (μ-law, A-law) was used for ($FLUT_3$) and ($FLUT_4$). The following configurations use the advanced spacing algorithms with linear interpolation described in this paper. $FLUT_7$ features an optimal LUT block (computed according to the method developed in [15] and summarized in section 3.1) coupled with a uniformly spaced codebook. $FLUT_6$ uses a codebook which follows the same spacing as the optimal LUT; note, however, that in this case optimality holds for the LUT block only and that the whole predistorter does not minimize the residual nonlinear distortion at the output of the amplifier. $FLUT_8$ features optimal LUT spacing and the new, improved codebook spacing method (see section 3.2). Furthermore a scenario where both the LUT and the codebook follow the sample equi-distribution principle, described in section 3.2, was also considered for comparison purposes ($FLUT_5$).

Comparative results for these predistorters are collected in figure 3a and 3b. Average power at the input of the amplifier varies from -21 dBm to -15 dBm. A very compact FLUT has been considered in order to fit the needs of high optical throughput (N_1 = 6; N_2 = 6 and L = 3). The FLUT was identified using a learning sequence of 2^{11} QPSK symbols with average input power P_{ref} = -18 dBm. NU spacing via μ-law and A-law (see TABLE 1 for the expression of the laws) were implemented for μ = 100 and A = 150 respectively. Trial and error seems to indicate that these values perform best. Results for basic OFDM (without predistortion) are also plotted for referencing purposes. We note that while conventional NU spacing algorithms outperform uniform spacing optimizing the LUT leads to a significant reduction in EVM. Mixing LUT optimization and an improved codebook brings further gain as one notes that $FLUT_8$ performs best.

IET Research Journals, pp. 1–6

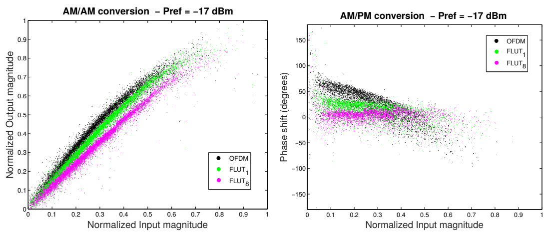

Fig. 4: AM-AM (left) and AM-PM (right) characteristics for an optical power of -17 dBm at SOA input for original system, compared to linearized systems $FLUT_1$, $FLUT_8$ with size $N_1 = N_2 = 6$.

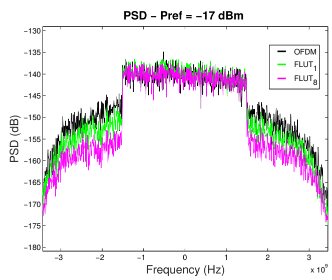

Fig. 5: Power Spectral Density of the received signal (original system and linearized systems $FLUT_1$, $FLUT_8$).

4.3 Influence of the Identification Power (P_{ref})

Figures 3a and 3b correspond to scenario where the FLUT parameters are identified for a fixed value of the input power and a power sweep is conducted to see how the various predistorters perform in a given range around this value. Another scenario involves re-identifying FLUT parameters for various values of the average input power. This is not unrealistic, in practice an FPGA implementation of the system could reasonably allow switching between various sets of parameters. The scenario is tested with P_{ref} varying from -23 dBm up to -13 dBm. The improvement in terms of EVM (Gain_{EVM}) for five FLUT variants is plotted in figure 3c. Note that, quite predictably, as the input power goes beyond a certain value saturation becomes such that predistorters no-longer manage to cope with the nonlinearities and Gain_{EVM} decreases sharply, with an EVM eventually exceeding the FEC* limit (assumed to correspond to an uncoded BER† of 10^{-3} [23]). However in the realistic power range featured in figure 3c FLUT_8 clearly outperforms other techniques. The effectiveness of this predistorter can also be assessed with the AM-AM and AM-PM characteristics, illustrated in figure 4, or in frequency domain where a reduced distortion can be observed both in-band and out-of-band (Fig. 5). At the considered input power $P_{ref} = -17$ dBm, FLUT_8 clearly outperforms FLUT_1 with performance still meeting the FEC limit.

4.4 Influence of the Henry Factor

Further investigation focused on the influence of amplitude-phase coupling in the SOA. The latter can be quantified by the Henry factor and has significant impact on the nonlinear behavior of the amplifier [22]. All previous results in the paper were obtained for a Henry factor α_H of 5. In the new scenario it varies from 1.52 to 7.6 with a step of 0.76. FLUT parameters are re-identified for each value of α_H. The results are collected in figure 3d. FLUT_8, once again, outperforms other variants.

4.5 FLUT Size

The size of the LUT and of the codebook are key parameters of the predistorter as they impact system complexity. In figures 3e-3f the performance of the various FLUT variants is tested varying N_1 and N_2 from 1 to 20 and 1 to 150 with $N_1 = N_2$ and keeping the same memory depth ($L = 3$). Beyond $N_1 = N_2 = 4$ the FLUT_8 outperforms other variants. It should be noted that for unrealistically high values of N_1 and N_2 (> 120) all variants tend to yield similar performance which is expected (figure 3f). Nonetheless, in a realistic scenario FLUT_8 offers a good performance/complexity trade-off.

5 Conclusion

The topic of digital predistortion has attracted significant attention in recent years. In the present paper the authors provided a comprehensive study for FLUTs testing several variants. A new method of non-uniform spacing was developed for the FIR codebook leading to a significant improvement in performance. It should be noted that the solution is particularly well adapted to optical systems. Its simplicity is well suited for optical data rates and no feedback loop is required. Indeed, in microwave systems one may be tempted to implement more complex, adaptive solutions featuring online computation that are simply not feasible in optical communications. Thus, a well designed FLUT appears all the more interesting.

6 References

1 H. Schmuck et al., "Demonstration of an SOA-assisted open metro- access infrastructure for heterogeneous services", *Opt. Express*, vol. 22, Issue 1, pp. 737-748, Jan. 2014.
2 S. Koenig et al., "Amplification of advanced modulation formats with a semiconductor optical amplifier cascade", *Opt. Express*, vol. 22, Issue 15, pp. 17854-17871, May 2014.
3 M. J. Connelly, Semiconductor Optical Amplifiers . Boston, MA:Kluwer, 2002.
4 P. B. Kennington, "High Linearity RF AmpliïňĄers Design." Norwood, MA: Artech House, 2000.
5 F. M. Ghannouchi, O. Hammi, and M. Helaloui, "Behavioral modeling and predistortion of wideband wireless transmitters," Wiley, 2015.
6 D. J. F. Barros and J. M. Kahn, "Optical modulator optimization for orthogonal frequency-division multiplexing," *J. Lightwave Technol.*, vol. 27, no. 13, pp. 2370-2378, July 2009.
7 Y. Bao, Z. Li, J. Li, X. Feng, B.O. Guan, and G. Li, "Nonlinearity mitigation for high-speed optical OFDM transmitters using digital pre-distortion", *Optics Express*, vol. 21, no. 6, pp. 7354-7361, Dec. 2013.
8 M. Faulkner and M. Johansson, "Adaptive linearization using predistortion. Experimental results," *IEEE Trans. Veh. Technol.*, vol. 43, no. 2, pp. 323-332, May 1994.
9 H. H. Chen, C. H. Lin, P. C. Huang, and J. T. Chen, "Joint Polynomial and Look-Up-Table Predistortion Power Amplifier Linearization," *IEEE Trans. on Circuits and Syst.-II*, vol. vol. 53, no. 8, pp. 612-616, Aug. 2006.
10 K. F. Liang, J. H. Chen, and Y. J. E. Chen, "A Quadratic-Interpolated LUT-Based Digital Predistortion Technique for Cellular Power Amplifiers," *IEEE Trans. on Circ. and Syst.-II*, vol. 61, no. 3, pp. 133-137, Mar. 2014.
11 J. K. Cavers, "Amplifier linearization using a digital predistorter with fast adaptation and low memory requirements," *IEEE Trans. Veh. Technol.*, vol. 39, no. 4, pp. 374-382, Nov. 1990.
12 A. Gersho, "Principles of quantization," *IEEE Trans. Circuits Syst.*, vol. CAS-25, no. 7, pp. 427-436, Jul. 1978.
13 J. Y. Hassani and M. Kamarei, "A flexible method of LUT indexing in digital predistortion linearization of RF power amplifiers," in *Proc. IEEE Int. Symp. Circuits Syst.*, vol. 1, pp. 53-56, May 2001.
14 S. Boumaiza, J. Li, M. J. Saidane, and F. Ghannouchi, "Adaptive Digital/RF predistortion using a nonuniform LUT indexing function with built-in dependence on the amplifier nonlinearity," *IEEE Trans. Microw. Theory Tech.*, vol. 52, no. 12, pp. 2670-2677, Dec. 2004.
15 S. N. Ba, K. Waheed, and G. T. Zhou, "Optimal spacing of a linearly interpolated complex-gain LUT predistorter," *IEEE Trans. Veh. Technol.*, vol. 59, no. 2, pp. 673-681, Feb. 2010.
16 S. S. Bouajina, M. J. Saidane, S. Boumaiza, and F. Ghannouchi, "A robust non-Uniform LUT indexing method in digital predistortion linearization of RF power amplifiers," *13th European Signal Processing Conference*, Antalya, 2005, pp. 1-4.
17 D. Selvadurai, R. M. Sidek, P. Varaham, and B. M. Ali, "A robust non-uniform indexation of a quadratically interpolated LUT predistorter for RF power amplifiers, " *12th Malaysia Int. Conf. on Communications*, Kuching, 2015, pp. 329-332.

* *Forward error correction*
† *Bit-error rate*

18 X. Feng, B. Feuvrie, A. S. Descamps, and Y. Wang, "Improved baseband digital predistortion for linearising PAs with nonlinear memory effects using linearly interpolated LUT, " *IEEE Electron. Lett.*, vol. 49, no. 22, pp. 1389-1391, Oct. 2013.
19 P. Jardin and G. Baudoin, "Filter lookup table method for Power amplifier linearization," *IEEE Trans. Veh. Technol.*, vol. 56, no. 3, pp. 1076-1087, May 2007.
20 S. Bejan, S. Azou, P. Morel, M. Telescu, N. Tanguy, and A. Sharaiha, "A Joint Linearization/Companding Approach for Improving a CO-OFDM Transmitter," *IEEE Photon. Technol. Lett.*, vol. 27, no. 20, pp. 2162-2165, Oct. 2015.
21 L. Sundstrom, M. Faulkner, and M. Johansson, "Quantization analysis and design of a digital predistortion linearizer for RF power amplifiers," *IEEE Trans. Veh. Technol.*, vol. 45, no. 4, pp. 707-719, Nov. 1996.
22 H. Khaleghi, P. Morel, A. Sharaiha, and T. Rampone, "Experimental validation of numerical simulations and performance analysis of a coherent optical-OFDM transmission system employing semiconductor optical amplifier," *J. Lightw. Technol.*, vol. 31, no. 1, pp. 161-170, Jan. 2013.
23 R. Schmogrow, B. Nebendahl, M. Winter, A. Josten, D. Hillerkuss, S. Koenig, J. Meyer, M. Dreschmann, M. Huebner, C. Koos, J. Becker, W. Freude, and J. Leuthold, "Error vector magnitude as a performance measure for advanced modulation formats," *IEEE Photon. Technol. Lett.*, vol. 24, no. 1, pp. 61-63, Jan. 2012.